Kovove Mater. 50 2012 259–268
DOI: 10.4149/km_2012_4_259

Evaluation of microstructure and fatigue properties of dissimilar AA7075/AA6061 joints produced by friction stir welding

F. Sarsılmaz[1], N. Ozdemir[2]*, I. Kırık[2]

[1] *University of Cumhuriyet, Faculty of Technical Education, Department of Machining, Sivas, Turkey*
[2] *University of Fırat, Faculty of Technical Education, Department of Metallurgy, 23119 Elazığ, Turkey*

Received 27 July 2011, received in revised form 4 October 2011, accepted 24 November 2011

Abstract

In this study, AISI 7075/AISI 6061 aluminum alloy plates were welded in butt position by friction stir welding (FSW). The welding process was performed using different process parameters, also investigating their effect on mechanical and fatigue behavior of FSW joints. The microstructural evolution of the material was analyzed by optical observations and SEM analysis of the weld cross sections. Tension tests were applied to welded parts to obtain the strength of the joints. Fatigue crack growth behavior and fatigue life of the welded joints have been evaluated by conducting the test using servo hydraulic controlled fatigue testing machine. According to the results, welding speed and tool profile in the tested range have major influence on the mechanical and fatigue properties of the FSW joints.

K e y w o r d s: fatigue lives, mechanical properties, friction stir welding

1. Introduction

Aluminum alloys with good heat transfer, high strength, good formability and weight saving have been considered for aerospace structure, shipbuilding, railway cars, etc. [1]. The ability to join aluminum alloys itself and to other materials with conventional fusion welding process such as gas tungsten, laser, electron beam welding opens up the possibility to product unexpected phase propagation and a series of negative metallurgical change occurs at the welding interface. Therefore, extensive care and precautions like pre and post heat treatment or quick welding speeds are required [2, 3]. These problems have been addressed by solid state welding processes, such as friction stir welding (FSW). Friction stir welding finds widespread industrial use as a mass production process for the joining of aluminum alloys. FSW is a relatively new technique developed by The Welding Institute (TWI) for the joining of aluminum alloys [4, 5]. FSW is one of the most popular welding techniques for joining Al-alloys. FSW is a solid-state process, which means that the base materials to be joined do not melt during the joining process. During FSW process, the rotating tool induces a complex deformation in the surrounding material that varies depending on the joining materials and welding conditions. Recrystallization of the microstructure takes place under severe plastic strain and elevated temperature due to FSW process, usually resulting in a very fine grained structure in the weld zone [5]. It is therefore expected that the complicated microstructure around the weld zone would strongly govern the fatigue properties of FS welds. There are several studies focusing on the fatigue behavior of the FS welds with welding flash or flaws such as void or "kissing bond" [6, 7]. FSW joints usually consist of four different regions. They are: (a) unaffected base metal, (b) heat affected zone (HAZ), (c) thermo-mechanically affected zone (TMAZ) and (d) friction stir processed (FSP) zone. The formation of above regions is affected by the material flow behavior under the action of rotating non-consumable tool. However, the material flow behavior is predominantly influenced by the FSW tool profiles, FSW tool dimensions and FSW process parameters [8, 9].

Fatigue is the principal cause of failure for welded joints in mechanical components; the application of FSW technology is in particular dependence on mech-

*Corresponding author: tel.: +90 424 2370000/4217; fax: +90 424 2184674; e-mail address: nozdemir@firat.edu.tr

Table 1. Chemical composition of test materials

Materials	Alloy elements (wt.%)						
	Cu	Fe	Si	Zn	Mn	Mg	Al
AA6061	0.15	0.6	0.8	0.1	0.1	1.1	Bal.
AA7075	1.3	0.45	0.4	5.5	0.3	2.4	Bal.

anical performances, which are strongly affected by the processing parameters. James et al. [10] showed the different fatigue behavior of two Al-Mg alloys as a function of welding speed. In addition, Ericsson et al. [11] and Somasekharan et al. [12] showed the variation of fatigue life of AA6082 joints with the welding speed, comparing the results with conventional fusion welding techniques. Al-Mg and Al-Mg-Si alloys plates of different thickness, joined with different welding speeds, have been studied also by Dickerson et al. [8]. The effects of welding parameters and tool profiles on FSP zone formation in dissimilar joints AA7075/AA6061 aluminum alloy are hitherto not reported. Hence, in this investigation an attempt has been made to understand the effect of tool pin profiles and traverse speed on mechanical and fatigue behavior. This paper presents the relation between the FSP zone formation and fatigue life of friction stir welded AA7075 to AA6061 aluminum alloy joints.

2. Materials and experimental procedure

In the experiments two kinds of aluminum alloy, standards AA7075 and AA6061 with dimensions $200 \times 100 \times 8\,\mathrm{mm}^3$, were used as test material. The nominal chemical compositions, physical properties and mechanical properties of test materials are given in Tables 1, 2 and 3, respectively. Non-consumable tools made of high-carbon steel have been used to fabricate the joints.

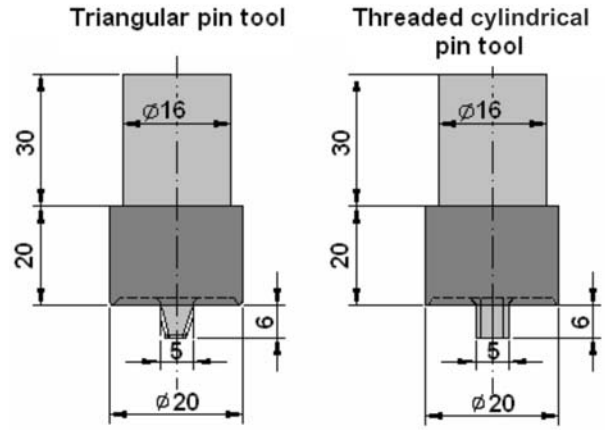

Fig. 1. Geometry and dimensions of stirrer tool.

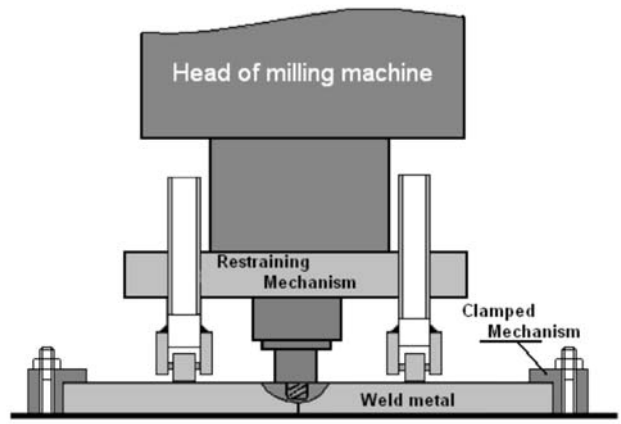

Fig. 2. Experimental set up.

Two different tool pin profiles, as shown in Fig. 1, have been used to fabricate the joints. The tool tilt angle was kept at 2.5 degree. Figure 2 shows the

Table 2. Mechanical properties of test materials

Materials	Tensile strength (MPa)	Yield strength (MPa)	Elastic modulus (GPa)	Hardness, HV
AA6061(T4)	235	140	70	70
AA7075(T6)	570	505	72	150

Table 3. Thermo-physical properties of test materials

Materials	Density ($\mathrm{kg\,m^{-3}}$)	Thermal expansion ($\mu\mathrm{m\,m^{-1}\,K^{-1}}$)	Electric conductivity (% IACS)	Thermal conductivity ($\mathrm{W\,m^{-1}\,K^{-1}}$)
AA6061(T4)	2700	23.3	40	155
AA7075(T6)	2810	23.5	33	134

Table 4. Process parameters used in FSW experiments

Sample No:	Stirrer profile	Rotational speed (rpm)	Traverse speed (mm min^{-1})
S1	Triangular	1120	160
S2			200
S3			250
S4		1400	160
S5			200
S6			250
S7	Treated cylindrical	1120	160
S8			200
S9			250
S10		1400	160
S11			200
S12			250

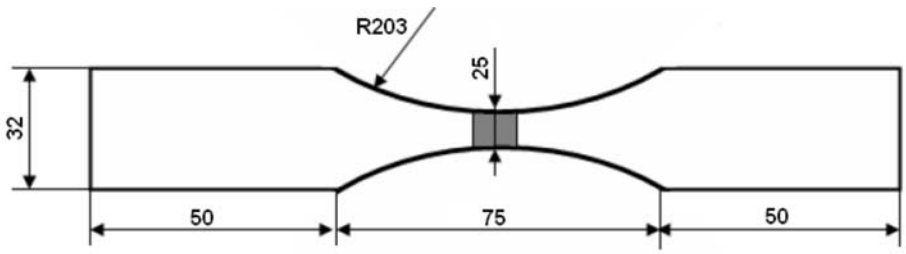

Fig. 3. Configuration and dimensions of fatigue test specimen (all dimensions in mm).

schematic presentation of a conventional milling machine, which was used to carry out FS welds. Using each tool, seven joints have been fabricated at three different rotational speeds and in three traverse speeds in this investigation. Table 4 shows the processing parameters used in FSW experiments.

The tensile test and fatigue specimens were prepared according to DIN 50109 and ASTM E466 standard, respectively (Fig. 3). High cycle fatigue tests have been performed on a resonant electro-mechanical testing machine in order to accelerate the testing time up to 250 Hz wave loading control. The Test-Tronic 50 ± 25 kN, produced by RUMUL, has been used.

The fatigue tests have been conducted in axial stress-amplitude control mode ($R = G_{\min}/G_{\max} = 0.1$) and at a frequency of 72 Hz. Eight groups of fatigue specimens were prepared to obtain *S-N* curves. Tensile testing was performed at room temperature using Instron type testing machine with 0.83×10^{-2} mm s^{-1} cross-head speed.

The visual inspections of the top surfaces of the friction stir welded specimens were not adequate to evaluate whether the friction stir welds quality was good or not. Therefore, conventional characterization techniques such as optical microscopy, scanning electron microscopy (SEM) were employed for studying the microstructure and mechanical properties of FSW. In order to determine microstructure properties of these joints, the specimens were cross-sectioned perpendicular to the weld interface using a low-speed saw. The cross-section of these joints was metallographically polished using diamond paste as final polish and then cleaned with acetone. Keller etchant was used for optical microstructure examination which solution consisted of 150 ml water, 3 ml nitric acid, 6 ml hydrofluoric acid, 6 ml hydrochloric acid, and was applied for 180 s.

3. Results and discussion

3.1. Microstructural evaluation

Figures 4 and 5 show an overview of the top surface of the friction stir welded AA6060/AA7075 alumina alloy, and show the surface appearances of each plate as a function of welding parameters. It can be clearly seen that there was no crack and voids on the top surface. Figures 6a and 7a illustrate light micrograph of traverse section through welded specimens produced using threaded cylindrical and triangular pin tool at a fixed travel speed of 1120 rpm, respectively. From the microstructural observations, the microstructures formed interface zone during or after FSW processes, there are four main different regions apparent in the interface zone of all the FSW joints. These main re-

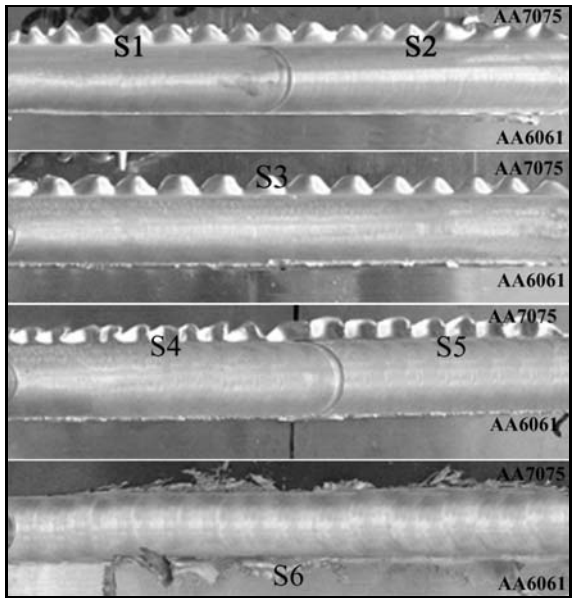

Fig. 4. The overview of the top surface of the friction stir welded of S1, S2, S3, S4, S5 and S6.

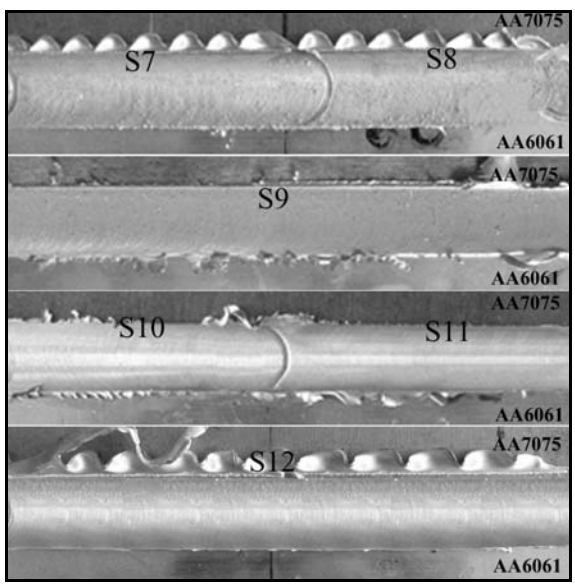

Fig. 5. The overview of the top surface of the friction stir welded S7, S8, S9, S10, S11 and S12.

gions were identified as parent metal (PM), HAZ, TMAZ and the dynamically re-crystallized stir zone (SZ). The boundary and shape of these regions were varied as a result of the relation between welding parameters such as rotational speed, traverse speed and tool-pin profile (Figs. 6b and 7b). Sato et al. [13] concluded that the shape of the weld zone depended on the welding parameters and thermal conductivity of the material.

The optical images were taken after immersion

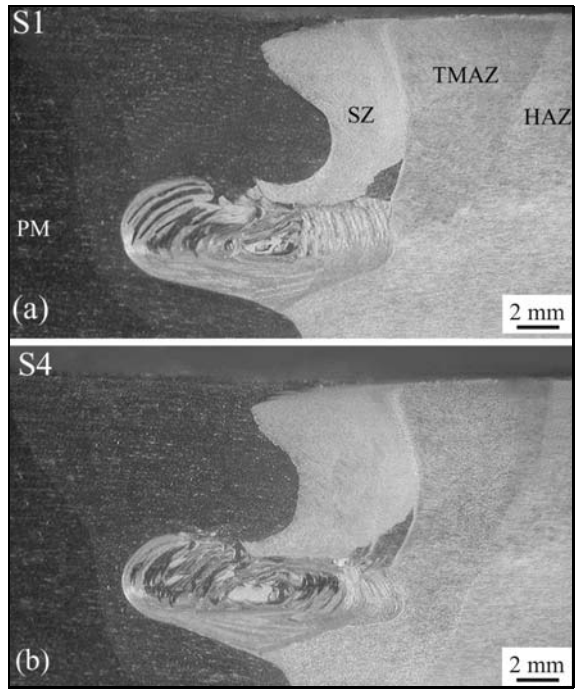

Fig. 6. Microstructure of the nugget zone: (a) the specimen welded at rotational speed 1120 rpm using triangular tool, (b) the specimen welded at rotational speed 1400 rpm using triangular tool.

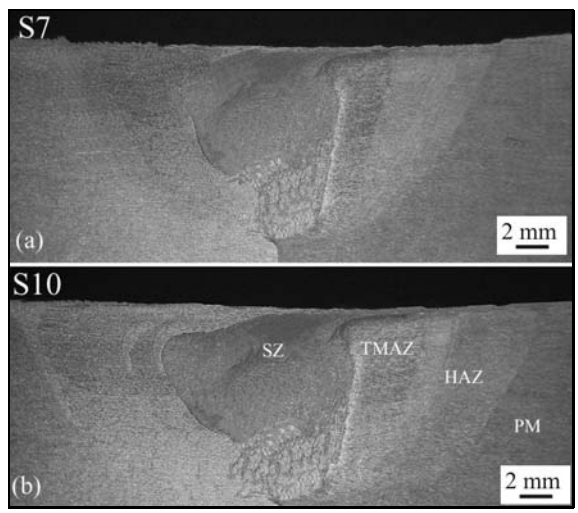

Fig. 7. Microstructure of the nugget zone: (a) the specimen welded at rotational speed 1120 rpm using treated cylindrical tool, (b) the specimen welded at rotational speed 1400 rpm using treated cylindrical tool.

of the specimens in $57\,g\,l^{-1}$ NaCl + $10\,ml\,l^{-1}$ H_2O_2 (30 vol.%) for 4 h followed by a brief treatment with Keller's reagent. It is evident that the welding parameters, especially rotation speed and traverse speed, affect the grain size in the nugget region of weld. At

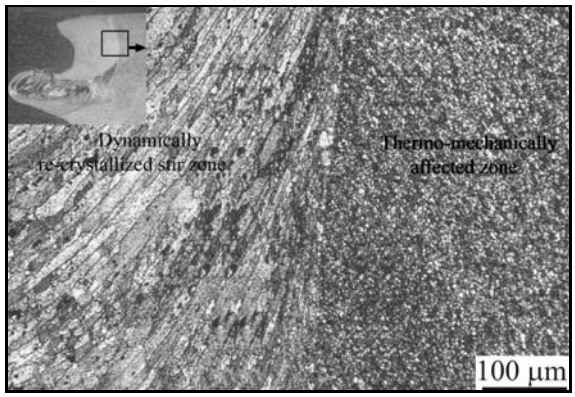

Fig. 8. Optical micrograph of the specimen welded at rotational speed 1120 rpm using triangular tool.

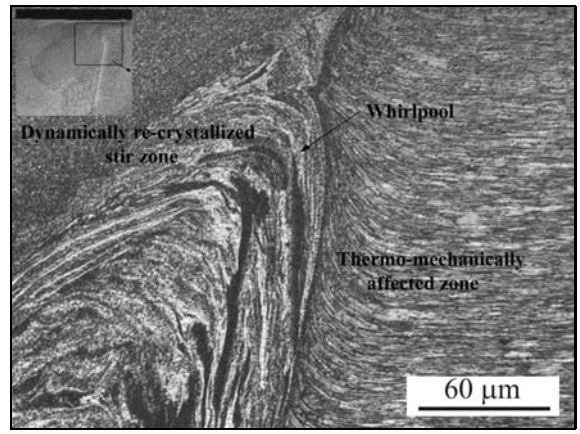

Fig. 9. Optical micrograph of the specimen welded at rotational speed 1120 rpm using treated cylindrical tool.

a fixed travel speed, an increase in rotation speed increases the grain size due to the higher heat input, while at fixed rotation speed; there is no change in grain size when changing the travel speed.

Figure 6 shows light micrograph of TMAZ and SZ taken from the interface zone of specimen S1 and S4. As shown in Fig. 6, in the specimen welded using threaded cylindrical pin, the boundary between TMAZ and SZ clearly separate from one another in a line which resembles a boot. This boot geometry formation was attributed to extreme deformation and frictional heat occurred between weldment and the tool pin. Fujii et al. [14] concluded that on the top surface the peak welding temperatures were almost the same for all the tool types. However, on the bottom surface the peak temperature for the triangular pin is lower than that for the others. Because the shoulder profile is the same for both the tool types, the temperatures near the shoulder on the top surface are almost the same, which proves that the heat input on the top surface is mainly focused on the shoulder. On the other hand, for the pin of triangular tool, the frictional area between the pin side and the welding material is limited to near the three sharp edges, which is much smaller than that of the threaded cylindrical tool. From the experimental results, it is thought that since larger frictional area must generate larger amount of friction heat, the friction heat generated by the triangular pin should be smaller than that by the threaded cylindrical pin. Consequently, for the triangular pin tool, the microstructural transformation is always lower than the threaded cylindrical pin. In the specimens of increasing rotational speed and low traverse speed, it was appeared high deformation level and as a result of this the grains tended to forge with coarsening.

From the micrograph of TMAZ taken at the interface zone of specimen welded at rotational speed 1120 rpm using triangular and threaded cylindrical pin tool, it is clear that the formation of structure usually showed fine equiaxed grains and ductility in TMAZ. The SZ had a fine equiaxed grain structure. This structure was produced by dynamic recrystallization, which was caused by frictional heat and severe plastic deformation (Figs. 8 and 9). The SZ also included "whirlpool" where the pin contacted the welded specimens. The whirlpool formation mechanism has been studied in recent papers. According to Fujii et al. [14] the whirlpool pattern was formed by the process of frictional heat due to rotation of the tool, in which forward movement extrudes metal around the retreating side of the tool. The whirlpool feature was observed in the stir zone and corresponded to the variation in the friction stir welding parameters [15, 16]. From the light micrograph taken at the weld zone of the all FSW specimens, it is seen that the shape of whirlpool formation appears similar to each other. The number of whirlpool decreased as the traverse speed increased. However, the whirlpool blank increased with increasing traverse speed. In addition, the parameters which generated higher frictional heat such as low traverse speed ($125\,\mathrm{mm\,min^{-1}}$) and high rotational speed (1400 rpm) exhibited wider weld nugget than other parameters. As a consequence of that, the microstructural transformation level of welding region increased proportionally.

3.2. Microhardness distribution

Figures 10–13 show the cross-sectional microhardness profiles of the friction stir welded joints in order to evaluate the material behavior as a function of the different welding parameters, respectively. As can be seen from these figures, almost the similar trend is observed in the microhardness profiles of all samples. The hardness of the SZ, TMAZ and HAZ increases with increasing rotational speed. This may be due to maintaining enough heat for dynamic recrystallization at

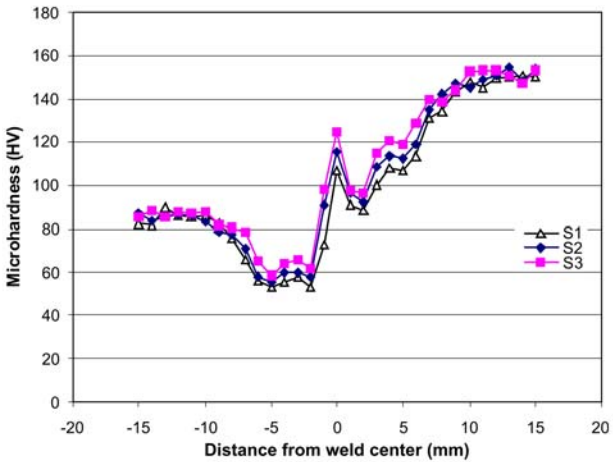

Fig. 10. Microhardness profile of specimens (S1, S2 and S3) using triangular tool.

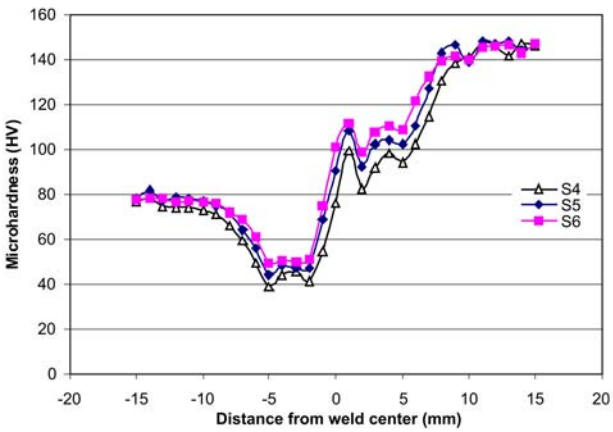

Fig. 11. Microhardness profile of specimens (S4, S5 and S6) using triangular tool.

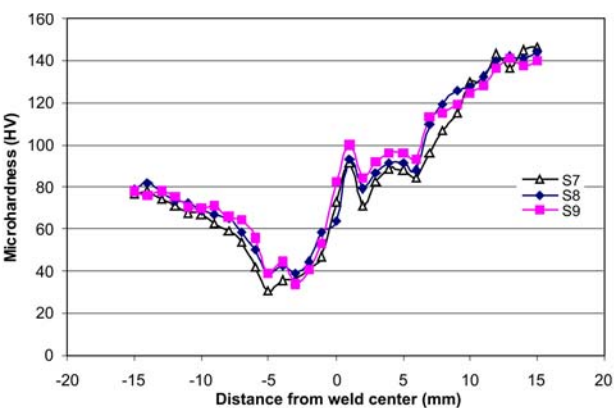

Fig. 12. Microhardness profile of specimens (S7, S8 and S9) using treated cylindrical tool.

higher tool rotation speed and grain refinement in the stir zone. At higher tool rotation speed (1400 rpm),

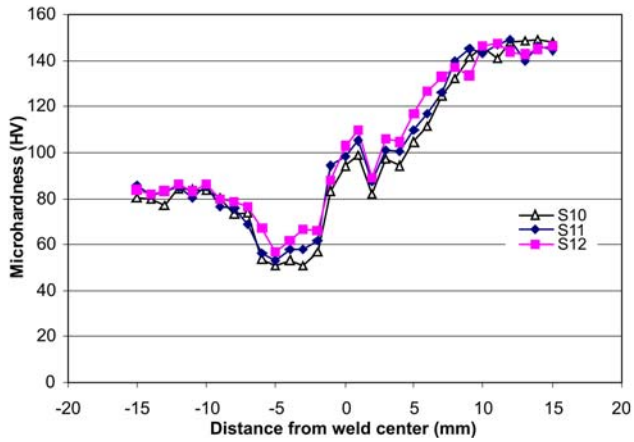

Fig. 13. Microhardness profile of specimens (S10, S11 and S12) using treated cylindrical tool.

an excessive heat generated by rotating pin causes decrease in the cooling rate which results in grain growth in the stir zone. This in turn causes decrease in the hardness. It can be seen that there were no substantial differences recorded with changing tool profile. But in stirred zone every group of samples demonstrated different hardness profile in each other with varying traverse and rotation speed. Especially for the samples (S3, S6, S9, S12) welded in 200 mm min^{-1} traverse speed, increasing was obtained in microhardness value. On the contrary, decreasing was occurred in microhardness by decreasing traverse speed gradually. This situation can be explained that the temperature amount reaches lower level with increasing traverse speed in weld zone. While structural formation was decreasing in dynamically recrystallized region, plastic deformation degree and stiffness reached high level due to extrusions intensity. This case confirms that the temperature and forging pressure are the most important factors on the microhardness properties in FSW process.

3.3. Tensile properties

Table 5 summarizes the mechanical properties (tensile stress and percentage elongation) of FSW joints for triangular pin and threaded cylindrical pin. Tensile strength linearly increased with increasing traverse speed. The fracture mainly occurred at the AA6061 side. From the tensile test results, it is observed that the FSW joints without defect exhibited better tensile properties than the defective joints. It is also observed that joint fabricated using threated cylindrical pin profile tool at the rotational speed of 1120 rpm and the welding speed of 250 mm min^{-1} exhibited superior tensile properties for 204 N mm^{-2} compared to the other joints. This result almost reached parent metal value 234 N mm^{-2}. Existing literature reports

Table 5. Mechanical properties for FSW welded samples, data acquired in tensile tests

Sample No:	Tensile strength ($N\,mm^{-2}$)	Elongation (%)
S1	137.3	9.48
S2	163.4	11.76
S3	196.2	12.79
S4	129.9	9.91
S5	144.6	8.41
S6	154.2	7.09
S7	159.8	12.40
S8	170.1	10.22
S9	204.2	14.92
S10	133.3	11.34
S11	149.5	9.81
S12	165.0	12.42

that, with the increase in traverse speed, improved mechanical properties have been observed. Increased tool rotational speed resulted in enhanced mechanical properties due to reduced porosity and grain size. This is because at higher tool rotational speed, an increased frictional heating and stirring is present which creates greater refinement of grain with more thorough material mixing and a uniform distribution of the grain in the parent material [17]. In the comprehending of the microstructural effects on fracture properties some SEM observations were performed on the fractured surfaces of the tested samples. Figure 14 shows that the fracture surface of the AA6061 plate tested in tension in the longitudinal direction was covered with a broad population of microscopic voids of different dimensions and shapes. At room temperature material showed some ductility with fracture and revealed local ductile characterization. The fractographic analysis of the tensile tested surfaces revealed that the size distribution of ductile dimples became more uniform and smaller on all observed surfaces at higher rotational and traverse speed but most constant by varying tool pin profile.

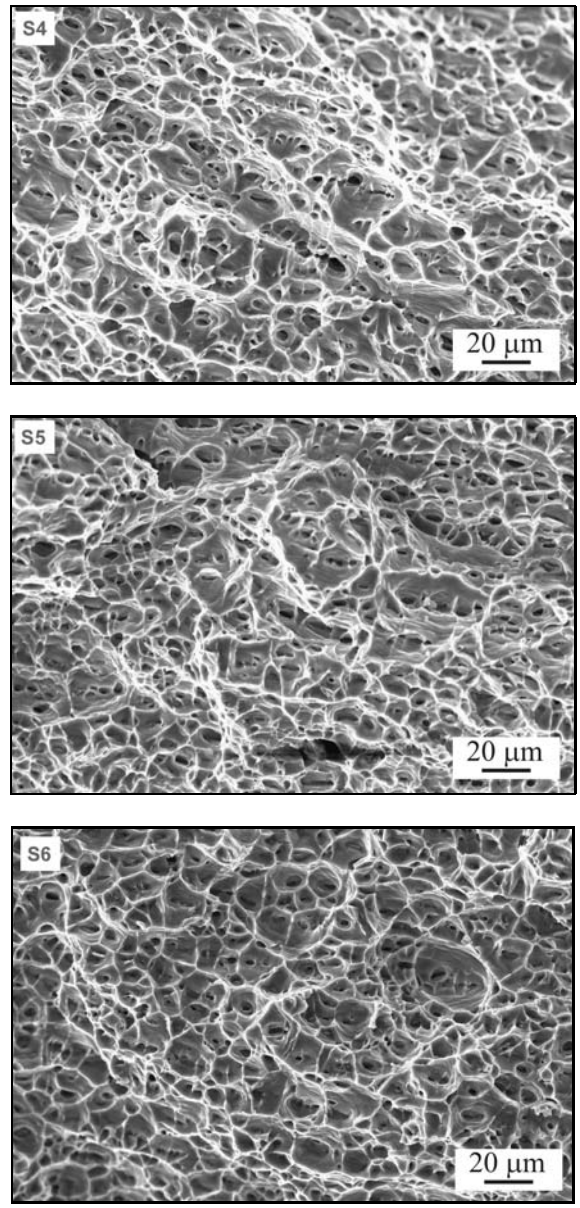

Fig. 14. SEM fractograph of the samples welded at 1400 rpm using triangular tool pin.

3.4. Evaluation of fatigue tests

Fatigue life of welded joints is determined by Wöhler curves. To determine start up tension in fatigue tests, fatigue experiments are calibrated by first applying high tensions to the specimens so as crack and break are seen at the low cycle values. Afterward, high cycle fatigue tests are applied to all specimens according to ASTM E-466 standard. Parameters chosen for literature compliant friction stir welded specimens are used in fatigue tests. Parameters are determined as Tension rate $R = 0.1$, Process frequency 72 Hz and pull-pull type, axial sinusoidal loaded fatigue test with constant amplitude load is applied to all joints. Resonant pin, electro-mechanic fatigue test machine is used in experiments. Logarithmic cycles corresponding to tension amplitude are considered at the fatigue limit values and cycle counts. These curves are converted to statistical data curves via ASCII codes existing in the fatigue test device. Curves sorted according to their process parameters are shown in Figs. 15–18, respectively.

Figures 15 and 16 show the *S-N* curves for fatigue test results of specimens joined using cylindrical and triangular tool pin revolving at rotational speed 1120 rpm. Additionally, fatigue resistance values listed by specimen codes and cycle counts achieved are

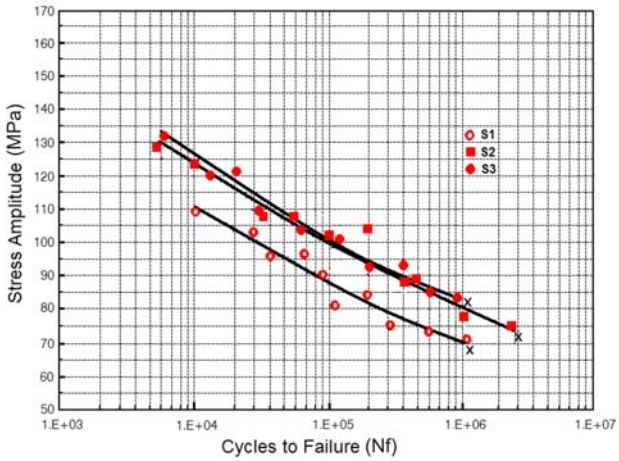

Fig. 15. S/N diagram for S1, S2 and S3 welded joints.

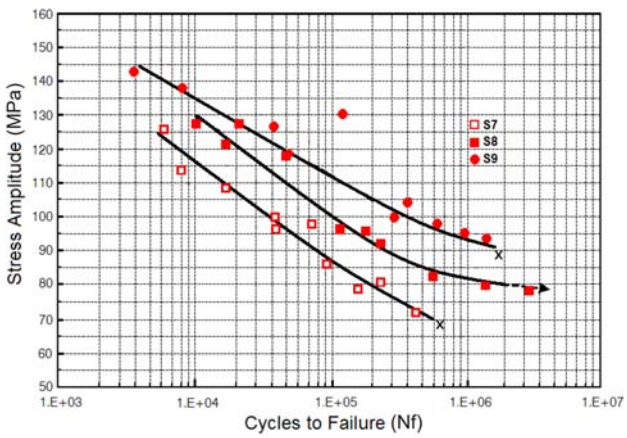

Fig. 16. S/N diagram for S7, S8 and S9 welded joints.

given in Table 6. Analyzing Wöhler curves of specimen S1, S2, S3, S7, S8 and S9 increases are seen in fatigue resistance limit values upon increasing traverse speeds. As a result of applied cycle, breaks are observed at all weldments made with triangular stir pin while all joints are broken except the specimen S8 which was joined with cylindrical stir pin. Among specimens joined at 1120 rev min^{-1}, maximum fatigue resistance is measured 91 MPa for specimen S9 which is joined at 250 mm min^{-1} traverse speed using cylindrical stir pin. Additionally, maximum fatigue resistance is measured as 84 MPa for specimens S4, S5 and S6 which are joined by triangular stir pins. As a result, all specimens joined using cylindrical stir pin show better resistance comparing to specimens joined using triangular stir pin.

Obviously, a cylindrical stir pin has more positive effect comparing to triangular stir pin in friction stir welding due to its impact on joining mechanism. The reason is the difference in stirring mechanism due to

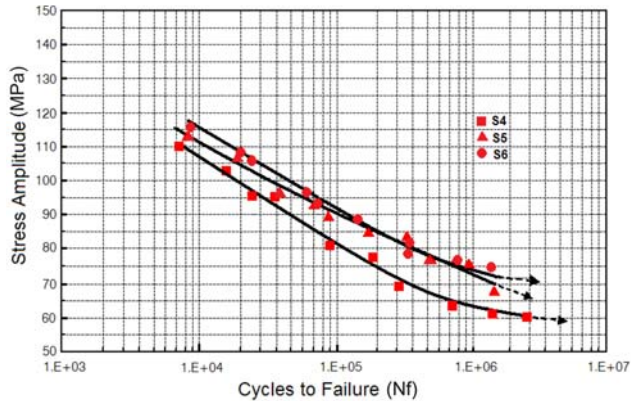

Fig. 17. S/N diagram for S4, S5 and S6 welded joints.

stir pin geometry. It is thought that, the triangular stir pin causes the joints to have shorter fatigue life and lower mechanical properties in joining materials because of inadequate stirring. It is known that the heat input degree has an important effect on the microstructural deformation and especially decrease in mechanical test values. The underlying reason of the gradual increase in fatigue resistance in parallel with traverse speeds is thought to be the temperature decrease. On the other hand, an extensive deformation in the deformed zone due to the increasing in the rotational speed could lead to build up of residual stresses [18]. In a previous study on residual stress of FSWed samples showed that [19], higher residual stresses at the interface can be attributed to the higher flow stress of the aluminum alloy. These residual stresses can also be thought to have an effect in the decrease of fatigue limit. The location of failure in all the cases was realized in the deformed zone.

S/N curves of specimens S4, S5, S6, S10, S11 and S12 joined at 1400 rpm rotational speed using cylindrical and triangular stir pin are given in Figs. 17 and 18. Analyzing curves of specimens S4, S5, S6 joined using triangular stir pin, 70 MPa fatigue resistance is obtained at the S6 specimen which is joined at the maximum traverse speed (250 mm min^{-1}). This value is measured as 68 MPa at the specimen S4 and 59 MPa at the specimen S5. Analyzing the results obtained so far, limit fatigue resistance values are decreasing following the gradual decrease in traveling speeds. The situation showed similar properties for specimens S10, S11, S12, which were joined using cylindrical stir pin. Fatigue resistance limit values of these specimens are determined 64, 68 and 73 MPa for specimens S10, S11 and S12, respectively. On the other hand, fatigue resistance of specimens joined using cylindrical pin are slightly higher than specimens joined using triangular pin according to their stir properties. These results, comparing to specimens joined under the same conditions but at 1120 rpm, show lower values obtained according to process temperatures.

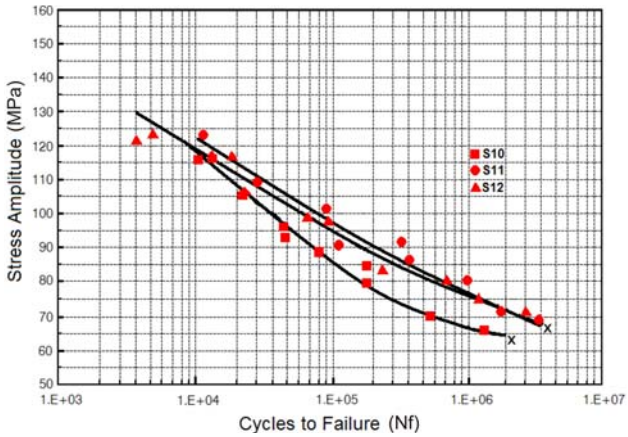

Fig. 18. S/N diagram for S10, S11 and S12 welded joints.

However, comparing both rotation speeds (1120 and 1400 rpm) according to traveling speed parameters, they show similar properties and good resistance values with increasing traverse speeds. As known, fatigue breaks are resulted from plastic deformation, pulling tension and fatigue cycled tension at the same time [10]. For this reason, fatigue cracks will not occur and develop in absence of these three factors. Conversion applied under specific tension amplitude causes deformation of the material and starts cracks while pulling tensions applied periodically are effective at developing these cracks. One fundamental factor affecting the fatigue mechanism in this direction is the plastic deformation [11]. Degree of the plastic deformation increases in specimens joined by friction stir weld at 1400 rpm because of high process temperature [20]. This situation decreases general mechanical properties of joints.

Fatigue resistance values of joints carried out at 1400 rpm rotational speeds are observed to be slightly lower than of those joined at 1120 rpm rotational speeds. The reason is thought to be high work temperature which significantly affects general mechanical properties at the joints since it extends the limits of structurally deformed zone at the welding zone. The fatigue resistance results obtained from S/N curves are consistent with literature. Analyzing impact of pin fatigue profiles on the fatigue performance, slight superiority of cylindrical stir pin comes forward in specimens joined at 1400 rpm. Experiment cycles are performed 3×10^6 cycles for all specimens joined using triangular stir pin before crack occurrence. Among the FSW joints joined using cylindrical stir pin, in specimens S10 and S11 cracks occurred while S12 did not crack.

4. Conclusions

In the study, the following generalizations are done based on joining AA6061 and AA7075 aluminum plates using friction stir welding, effect of stir pin geometry and traveling speed on fatigue behavior and related results.

1. The present study has demonstrated that AA6061 and AA7075 aluminum alloy plates are joined successfully in butt position using friction stir welding technique with two stir pins which have different geometry (cylindrical and triangular). Welded joints and weld seams are observed to be much smoother comparing to other welding methods and residues, spaces or unconnected points are not seen on joint surface.

2. From the results of microstructure analyses and mechanical test, it is clear that welding properties, such as the microstructure and fatigue life, were strongly influenced by traverse speed and tool profile. Especially, by choosing rotational speed, traverse speed and tool profile properly, it is possible to increase the quality of joint.

3. The best fatigue endurance is measured for specimen S9 as 91 MPa according to fatigue test results. Comparing these values according to their pin profiles, the cylindrical pin shows better resistance comparing to the triangular pin profile. Analyzing from the revolution count perspective, independent of the profile used for welding, resistance of 1120 rpm welds is slightly higher than that done at 1400 rpm welding. Taking traveling speeds into account within their parameter group, FSW joints produced using maximum traveling speeds show good results.

Acknowledgements

The authors would like to thank the University of Fırat for financial support of investigations. This work is sponsored by University of Fırat Research Fund under the project No: 1250.

References

[1] Davis, C. J., Thomas, W. M.: Welding Journal, *75*, 1996, p. 41.
[2] Sarsilmaz, F.: Investigation of Microstructure and Mechanical Properties of Friction Stir Welded AA7075 /AA6061. [Ph.D. Thesis]. Elazig, University of Firat 2008.
[3] Thomas, W. M., Nicholas, E. D.: Materials Design, *18*, 1997, p. 269. doi:10.1016/S0261-3069(97)00062-9
[4] Uzun, H.: Materials and Design, *28*, 2007, p. 1440. doi:10.1016/j.matdes.2006.03.023
[5] Cavaliere, P., Cerri, E.: Journal of Materials Science, *40*, 2005, p. 3669. doi:10.1007/s10853-005-0474-5
[6] Kim, Y. G., Fujii, H., Tsumura, T., Komazaki, T., Nakata, K.: Materials Letters, *60*, 2006, p. 3830. doi:10.1016/j.matlet.2006.03.123
[7] Cavaliere, P., Nobile, R., Panella, F. W., Squillace, A.: Materials Characterization, *57*, 2006, p. 100. doi:10.1016/j.matchar.2005.12.015

[8] Dickerson, T. L., Przydatek, J.: International Journal of Fatigue, *25*, 2003, p. 1399. doi:10.1016/S0142-1123(03)00060-4
[9] Mishra, R. S., Ma, Z. Y.: Materials Science Engineering R., *50*, 2005, p. 1. doi:10.1016/j.mser.2005.07.001
[10] James, M. N., Hattingh, D. G., Bradley, G. R.: International Journal of Fatigue, *25*, 2003, p. 1389. doi:10.1016/S0142-1123(03)00061-6
[11] Ericsson, M., Sandstrom, R.: International Journal of Fatigue, *25*, 2006, p. 1379. doi:10.1016/S0142-1123(03)00059-8
[12] Somasekharan, A. C., Murr, L. E.: Materials Characterization, *52*, 2004, p. 49. doi:10.1016/j.matchar.2004.03.005
[13] Sato, Y. S., Yamanoi, H., Kokawa, H., Furuhara, T.: Scripta Materialia, *57*, 2007, p. 557. doi:10.1016/j.scriptamat.2007.04.050
[14] Fujii, H., Cui, L., Maeda, M., Nogi, K.: Materials Science and Engineering: A, *419*, 2006, p. 25. doi:10.1016/j.msea.2005.11.045
[15] Ouyang, J., Yarrapareddy, E., Kovacevic, R.: Journal of Materials Processing Technology, *172*, 2006, p. 110. doi:10.1016/j.jmatprotec.2005.09.013
[16] Liu, H. J., Chen, Y. C., Feng, J. C.: Scripta Materialia, *55*, 2006, p. 231. doi:10.1016/j.scriptamat.2006.04.013
[17] Elangovan, K., Balasubramanian, V.: Journal of Materials Processing Technology, *200*, 2008, p. 163. doi:10.1016/j.jmatprotec.2007.09.019
[18] Lemmen, H. J. K., Alderliesten, R. C., Benedictus, R.: International Journal of Fatigue, *32*, 2010, p. 1928. doi:10.1016/j.ijfatigue.2010.06.001
[19] Bussu, G., Irwing, P. E.: International Journal of Fatigue, *25*, 2003, p. 77. doi:10.1016/S0142-1123(02)00038-5
[20] Meran, C.: Materials & Design, *27*, 2006, p. 719. doi:10.1016/j.matdes.2005.05.006